Original Research

Pediatric Perfusion Imaging Using Pulsed Arterial Spin Labeling

Jiongjiong Wang, PhD,[1,2]* Daniel J. Licht, MD,[3] Geon-Ho Jahng, PhD[4]
Chia-Shang Liu, BA,[5] Joan T. Rubin, BA,[6] John Haselgrove, PhD,[6]
Robert A. Zimmerman, MD,[6] and John A. Detre, MD[1,2]

Purpose: To test the feasibility of pediatric perfusion imaging using a pulsed arterial spin labeling (ASL) technique at 1.5 T.

Materials and Methods: ASL perfusion imaging was carried out on seven neurologically normal children and five healthy adults. The signal-to-noise ratio (SNR) of the perfusion images along with T1, M_0, arterial transit time, and the temporal fluctuation of the ASL image series were measured and compared between the two age groups. In addition, ASL perfusion magnetic resonance (MR) was performed on three children with neurologic disorder.

Results: In the cohort of neurologically normal children, a 70% increase in the SNR of the ASL perfusion images and a 30% increase in the absolute cerebral blood flow compared to the adult data were observed. The measures of ASL SNR, T1, and M_0 were found to decrease linearly with age. Transit time and temporal fluctuation of the ASL perfusion image series were not significantly different between the two age groups. The feasibility of ASL in the diagnosis of pediatric neurologic disease was also illustrated.

Conclusion: ASL is a promising tool for pediatric perfusion imaging given the unique and reciprocal benefits in terms of safety and image quality .

Key Words: arterial spin labeling (ASL); pediatric brain imaging; cerebral blood flow (CBF); pediatric stroke; periventricular leukomalacia (PVL); benign external hydrocephalus
J. Magn. Reson. Imaging 2003;18:404–413.

[1]Department of Radiology, University of Pennsylvania, Philadelphia, Pennsylvania.
[2]Department of Neurology, University of Pennsylvania, Philadelphia, Pennsylvania.
[3]Department of Child Neurology, the Children's Hospital of Philadelphia, Philadelphia, Pennsylvania.
[4]VA Medical Center, University of California-San Francisco, San Francisco, California.
[5]Department of Biochemistry and Biophysics, University of Pennsylvania, Philadelphia, Pennsylvania.
[6]Department of Radiology, the Children's Hospital of Philadelphia, Philadelphia, Pennsylvania.
Contract grant sponsor: W.W. Smith Charitable Trust; Contract grant number: H0203; Contract grant sponsor: Pfizer.
*Address reprint requests to: J.W., Department of Neurology, University of Pennsylvania, 3400 Spruce Street, Philadelphia, PA 19104. E-mail: jwang@rad.upenn.edu
Received January 13, 2003; Accepted May 16, 2003.
DOI 10.1002/jmri.10372
Published online in Wiley InterScience (www.interscience.wiley.com).

CEREBRAL BLOOD FLOW (CBF) represents an important physiologic parameter for the diagnosis and management of childhood brain disorders, particularly cerebrovascular disease. To date, however, both normative and disease data on pediatric brain perfusion remain sparse due to the lack of suitable techniques for CBF measurement. Nuclear medicine approaches, such as single positron emission computed tomography (SPECT) and positron emission tomography (PET), rely on radioisotopes and are ethically problematic when applied to the pediatric population. Although dynamic tracking of paramagnetic contrast agent in conjunction with magnetic resonance imaging (MRI) scanning has been routinely conducted in adults to measure cerebral perfusion(1), its application in children has been limited by the technical difficulty in administering the intravenous contrast agent, especially in neonates. While macrovascular flow can be assessed using transcranial Doppler ultrasound or phase contrast MR angiography, only large vessels can be detected and flow values do not reliably predict CBF.

Arterial spin labeling (ASL) perfusion MRI is a promising approach to directly measure CBF by utilizing arterial blood water as an endogenous diffusible tracer, in a way analgous to that used in ^{15}O PET scanning(2). In ASL, arterial blood water is magnetically labeled proximal to the tissue of interest, and the effects of this pre-labeling are determined by pair-wise comparison with images acquired using control labeling. This technique has been demonstrated to provide reproducible and reliable quantitative CBF measurements in various cerebrovascular and psychiatric disorders in adults(3–5). Pediatric perfusion imaging based on ASL may provide unique advantages compared to applications of ASL in the adult population. Because ASL is totally noninvasive and does not require intravenous injection, pediatric perfusion can be safely assessed in a wide range of age groups, including adolescents, children, neonates, and even fetuses. While the widespread application of ASL in the adult (especially aged) population has been hampered by the relatively small fractional perfusion signal, pediatric ASL is expected to provide improved signal-to-noise ratio (SNR) due to the increased blood flow in children(6–12). Previous evidence also suggested that the water content of brain is higher in children than in adults(13), resulting in in-

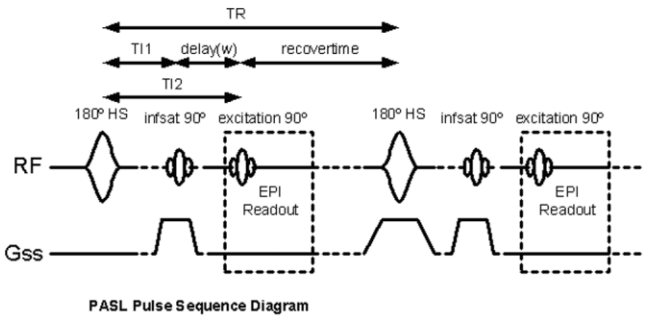

Figure 1. Diagram of the PASL pulse sequence used in the present study, depicting related RF pulses and the gradients along the slice direction (Gss). The pulse sequence consisted of interleaved global and slice-selective inversion recovery acquisitions using HS pulses. Saturation pulses were applied to a slab inferior to the imaging slice (infsat 90°) to externally define the duration of the tagging bolus (TI_1), followed by a post-labeling delay time (w). Image acquisition was carried out at TI_2 after the HS inversion pulses using gradient-echo EPI sequences.

creased equilibrium MR signal and spin-lattice, spin-spin relaxation time (T1, T2)(14), which should further improve ASL signal in children through increased tracer concentration and life time. Given the unique and reciprocal benefits in terms of safety and image quality, ASL perfusion MRI may be particularly well suited for pediatric imaging.

The present study was intended to test the feasibility of pediatric perfusion imaging using a pulsed ASL (PASL) technique at 1.5 T. Compared to continuous ASL, which employs relatively long width radiofrequency (RF) pulses, PASL techniques use nearly instant pulses with comparatively low levels of RF deposition for spin labeling, and are particularly advantageous in circumstances where specific absorption rate (SAR) imposes a limitation, such as high magnetic field and pediatric imaging(15). The second purpose of this study was to test the hypothesis that pediatric ASL provides improved SNR, as well as increased measures of CBF, compared to adult data. We compared PASL perfusion images in children diagnosed without neurologic disease and healthy adults by examining parameters including T1, M_0, ASL SNR, CBF, and arterial transit time. Temporal fluctuation of the perfusion image series was also measured because previous functional MRI studies suggested that child data may contain higher level of motion and physiologic noise(16). Finally, selected children with neurologic diseases were scanned using the PASL technique to illustrate its feasibility in the diagnosis of pediatric brain disorders.

MATERIALS AND METHODS

Imaging Sequence

MR scanning was carried out on a 1.5-T Siemens Vision whole body scanner, using the standard birdcage head coil. Figure 1 displays the diagram of the PASL pulse sequence. This technique was a modified version of the FAIR technique(17), in which a saturation pulse was applied at TI_1 = 800 msec after the global or slice-selective inversion(18). For optimal labeling, a hyperbolic secant (HS) inversion pulse was generated using the MATPULSE software(19) with 15.36-msec duration, 22 μT RF amplitude, and 95% tagging efficiency. A gradient of 0.7 mT/m was applied along with the HS pulse during tag, while the HS pulse was applied in the absence of gradient during control. The slab of the slice-selective inversion was 10-cm thick, and the slice profile was verified by Bloch equation simulation as well as phantom test. The saturation pulse was applied to a 10-cm slab adjacent and inferior to the selective inversion slab in both label and control acquisitions. The purpose of this saturation pulse was to eliminate any remaining labeling effect at TI_1, so that the duration of the tagging bolus could be explicitly defined for perfusion quantification(20). To improve the effect for spoiling longitudinal magnetization, two saturation pulses were played out consecutively followed by crusher gradients. A delay time (w) was inserted between the saturation and excitation pulses to minimize transit related effects in ASL images(20,21). This delay time should be greater than the arterial transit time to allow all the labeled blood to flow into image slices by the time image is acquired (TI_2), thereby the ASL perfusion measurement would be immune to uncertainties in arterial transit time. Imaging parameters were: matrix size = 64 × 64, TR/TE = 3000/29 msec, slice thickness = 8 mm with 2-mm gap. Seven slices were acquired sequentially from inferior to superior using a gradient-echo echo-planer imaging (EPI) sequence, and each slice acquisition took about 80 msec. The field of view (FOV) was varied from 20–22 cm in children and 22–24 cm in adults, which could cause about 20% SNR gain for adult data.

MR Scanning

Perfusion scans were performed on five healthy adults (one woman and four men, ages 27–40 years, mean 31.6 years) and nine children (one girl, ages one month to 10 years, mean 3.7 years). The pediatric subjects were identified from a list of patients scheduled for clinical non-contrast MRI for the diagnosis of developmental delay and headaches. The pediatric perfusion scans (about 13 minutes) were attached to the routine clinical examination, during which vital physiologic parameters were continuously monitored. Written informed consent was obtained from the children's parents as well as from adults before the scan according to an Institutional Review Board approval. Two children's data were later excluded because of RF artifact, resulting in seven complete pediatric data sets. Steady state perfusion imaging with 80 acquisitions was performed at three delays, respectively, on each adult and child (w = 0.1, 0.4, and 0.7 seconds in all adults, and five children; w = 0.3, 0.6, and 0.9 seconds in the remaining two children). A M_0 image was acquired after the perfusion scans for T1 mapping. Five of the seven children (age < 5) were sedated during the scan. In addition, the perfusion protocol was carried out on three children with diagnosed neurologic diseases (periventricular leukomalacia, benign external hydrocephalus, and stroke).

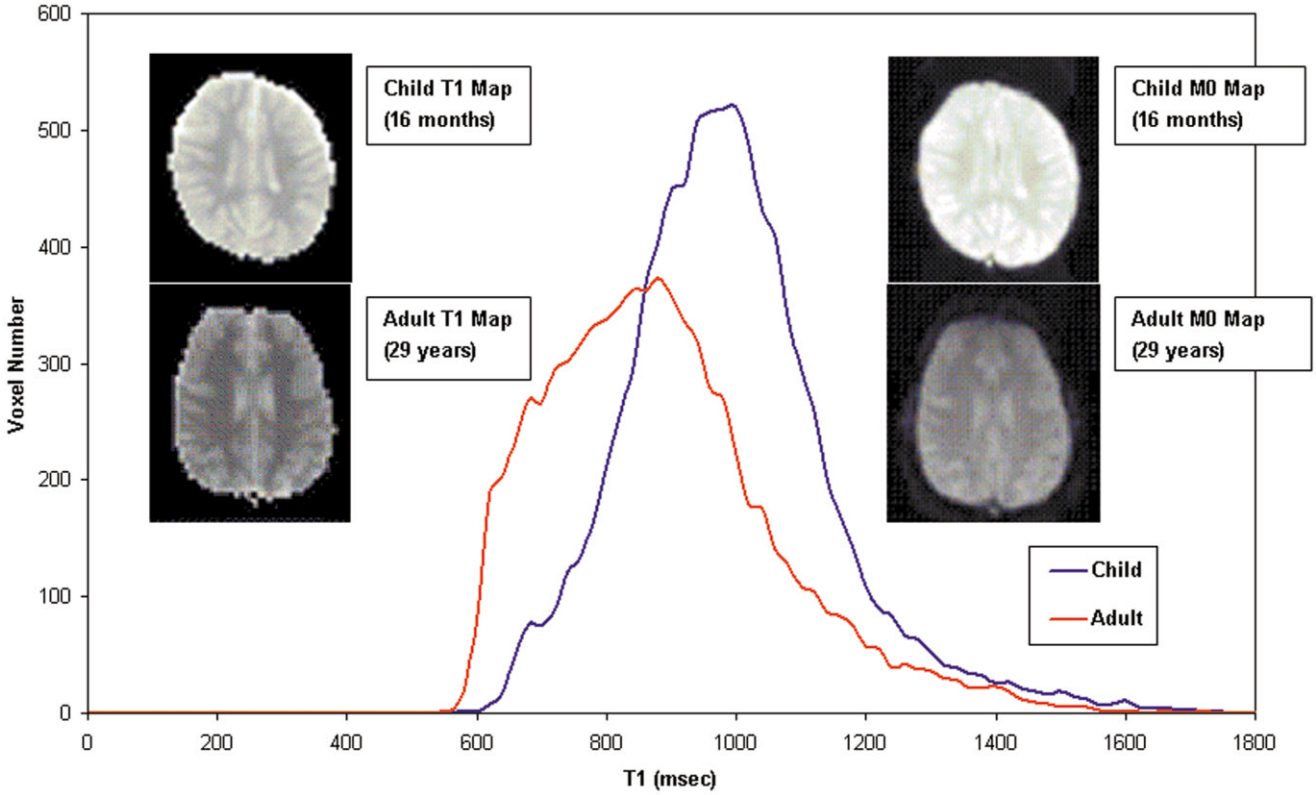

Figure 2. T1 histogram averaged across the seven children and five adults with representative T1 and M_0 images acquired in a 16-month-old child and 29-year-old adult (displayed using same scale). The child T1 and M_0 images have higher intensities than adult images.

Data Processing

The raw image series at each delay were separated into label and control pairs and pair-wise subtracted, followed by averaging across the image series to form the mean ASL perfusion images. The first pair of acquisition was excluded from analysis to avoid saturation effect. In each child or adult, T1 image was calculated using the M_0 image and mean raw image in perfusion scans. Due to the employed TR of three seconds, this T1 measurement may cause underestimation of prolonged T1 values greater than one second, e.g., 14% reduction for T1 of 1.4 seconds. Visual inspection of the ASL images at different delay times suggested most of the intravascular focal signals disappeared at $w \geq 0.7$ seconds (see Fig. 2); therefore, data acquired at $w = 0.7$ second were used for CBF quantification. Linear interpolation was used to obtain the data at $w = 0.7$ second in the two children undergoing scans with $w = 0.3$, 0.6, and 0.9 seconds. CBF images were calculated by (18)

$$f = \frac{\lambda \Delta M}{2\alpha M_0 TI_1 \exp(-TI_2/T_{1a})} \quad (1)$$

where ΔM is the difference signal between tag and control acquisitions, λ is the blood/tissue water partition coefficient, T_{1a} is the longitudinal relaxation time of blood, α is the inversion efficiency, $TI_1 = 800$ msec is the duration between the inversion and saturation pulses, TI_2 ($= TI_1 + w$) is the image acquisition time (see Fig. 1). Conversion to CBF values used assumed values of $\lambda = 0.9$ mL/g, $\alpha = 0.95$, $T_{1a} = 1.2$ seconds, and the acquired M_0 image. These parameters were primarily based on experience in healthy adults; potential effects of ignoring the difference between adults and children on CBF quantification will be discussed below.

Because ASL signal series at three delays were acquired in each child or adult, it is possible to estimate the arterial transit time for the tagged blood to flow from the labeling region to the imaging slices. This was per-

Table 1
Whole Brain Mean T1 and M0 Along With the Gray and White Matter Fraction in Child and Adult Groups

	T1 (msec)	M_0 (AU)	Gray matter fraction	White matter fraction
Child group	988.1 ± 59.0	1168.2 ± 204.7	0.73 ± 0.07	0.17 ± 0.09
Adult group	885.3 ± 29.7	946.8 ± 44.3	0.52 ± 0.03	0.30 ± 0.06
T test *P* value (2-tailed unpaired)	0.003	0.029	0.0006	0.01

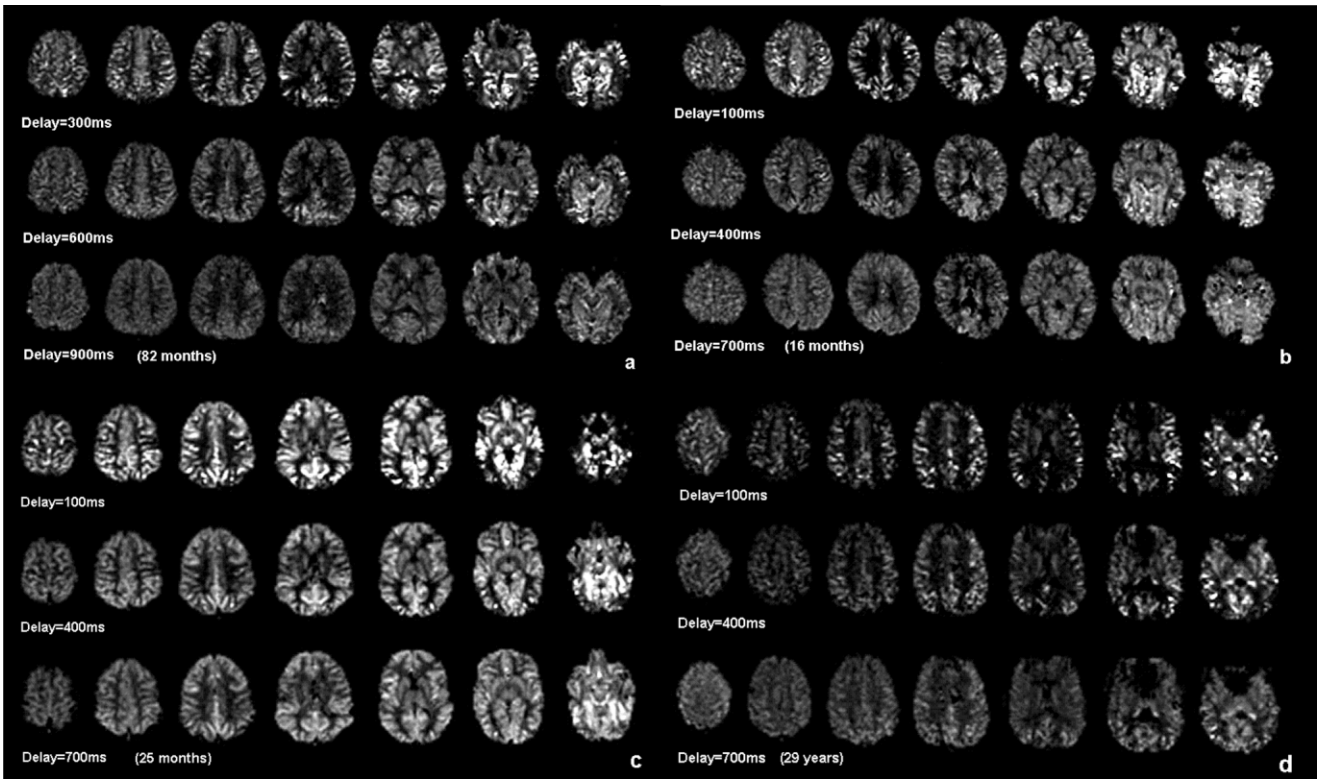

Figure 3. Four representative sets of ASL perfusion images acquired at three delays in the child (**a**, **b**, **c**) and adult (**d**) group.

formed by fitting the ASL signal series with the following equation using the "curvefit" routine supplied by Interactive Data Language(18)

$$\Delta M = \frac{-2M_0 f\alpha}{\lambda} \exp(-TI_2/T_{1a}) \times [\min(\delta_a - w, 0) - (\delta_a - TI_2)] \quad (2)$$

where δ_a is transit time and the min( ) function returns the smaller of its two arguments. Figure 5a displays the simulation results of Eq. [2] (fractional ASL signal, $\Delta M/M_0$, as a function of delay time, w) at different assumed transit times. The parameters used in the simulation were $f = 60$ mL/100 g/minute, $\lambda = 0.9$ mL/g, $\alpha = 0.95$, $T_{1a} = 1.2$ seconds, and $TI_1 = 800$ msec. It can be seen that ΔM reaches the maximum at $w = \delta_a$ and at least one sample point has to be acquired at $w < \delta_a$ for convergent results. Analyses of the data showed only the ASL signals in the bottom slice met the criteria in all the subjects and were used to estimate the transit time. In two children, the ASL signals in the two edge slices were found to be higher than the center five slices, which is suspected to be caused by an imperfect slice profile of the labeling pulse perhaps attributable to suboptimal coil performance. Data from the two edge slices of these two children were excluded for transit time measurement and other analyses. In each child or adult, two regions of interest (ROI) of gray and white matter were identified based on the T1 range associated with each type of tissue according to the T1 images and histogram (see Fig. 1). We chose to empirically define the segmentation of gray and white matter mainly because automatic segmentation (SPM) failed to reliably separate different tissue type in child data. Comparison

Table 2
Demographic Data as Well as Perfusion Measurements of the Child Group

Child subject	Age (months)	Gender	ASL SNR (AU)			CBF (mL/100g/min)		
			GM	WM	WB	GM	WM	WB
1	82	M	7.53	2.99	6.24	75.4	33.3	65.1
2	120	M	7.06	2.11	5.81	64.6	19.2	54.3
3	16	M	7.19	2.49	7.01	70.1	27.7	68.4
4	57	M	7.25	3.66	6.70	67.3	41.0	63.4
5	20	M	13.5	6.03	12.5	99.3	44.7	92.7
6	17	M	8.71	6.02	8.55	54.2	36.4	52.0
7	1	F	7.23	3.60	6.18	64.1	33.1	55.0
AVG ± SD	44.7 ± 43.4		8.35 ± 2.34	3.84 ± 1.59	7.57 ± 2.35	70.7 ± 14.1	33.6 ± 8.4	64.4 ± 13.9

GM = gray matter, WM = white matter, WB = whole brain.

Table 3
Demographic Data as Well as Perfusion Measurements of the Adult Group

Adult subject	Age (years)	Gender	ASL SNR (AU)			CBF (mL/100g/min)		
			GM	WM	WB	GM	WM	WB
1	27	M	5.35	1.87	4.19	44.5	16.2	36.2
2	29	M	6.27	3.62	5.43	55.7	33.5	50.0
3	31	F	5.59	1.48	4.68	69.9	17.2	61.4
4	31	M	4.40	1.88	3.79	46.9	21.5	42.5
5	40	M	4.67	2.16	3.95	71.5	36.6	63.3
AVG ± SD	31.6 ± 5.0		5.26 ± 0.74	2.20 ± 0.82	4.41 ± 0.66	57.7 ± 12.5	25.0 ± 9.4	50.7 ± 11.7
P(T test)			0.01	0.04	0.01	0.12	0.14	0.09

GM = gray matter, WM = white matter, WB = whole brain.

between the adult and child groups was then performed on the whole brain and ROI based measures of ASL SNR, M_0, T1, CBF, and transit time. Because the apparent intensities of M_0 images are affected by MR system variations, the M_0 values were calibrated using recorded transmitter voltage and receiver gain on each subject according to the product manual(22). The ASL SNR was defined as the ASL signal intensity divided by the background noise level (measured from regions of no signal). These parameters were then entered for regression analysis with age using SPSS software as well as an unpaired *t*-test (two-tailed) for comparison between the child and adult group. In addition, the temporal stability of the perfusion image series, determined

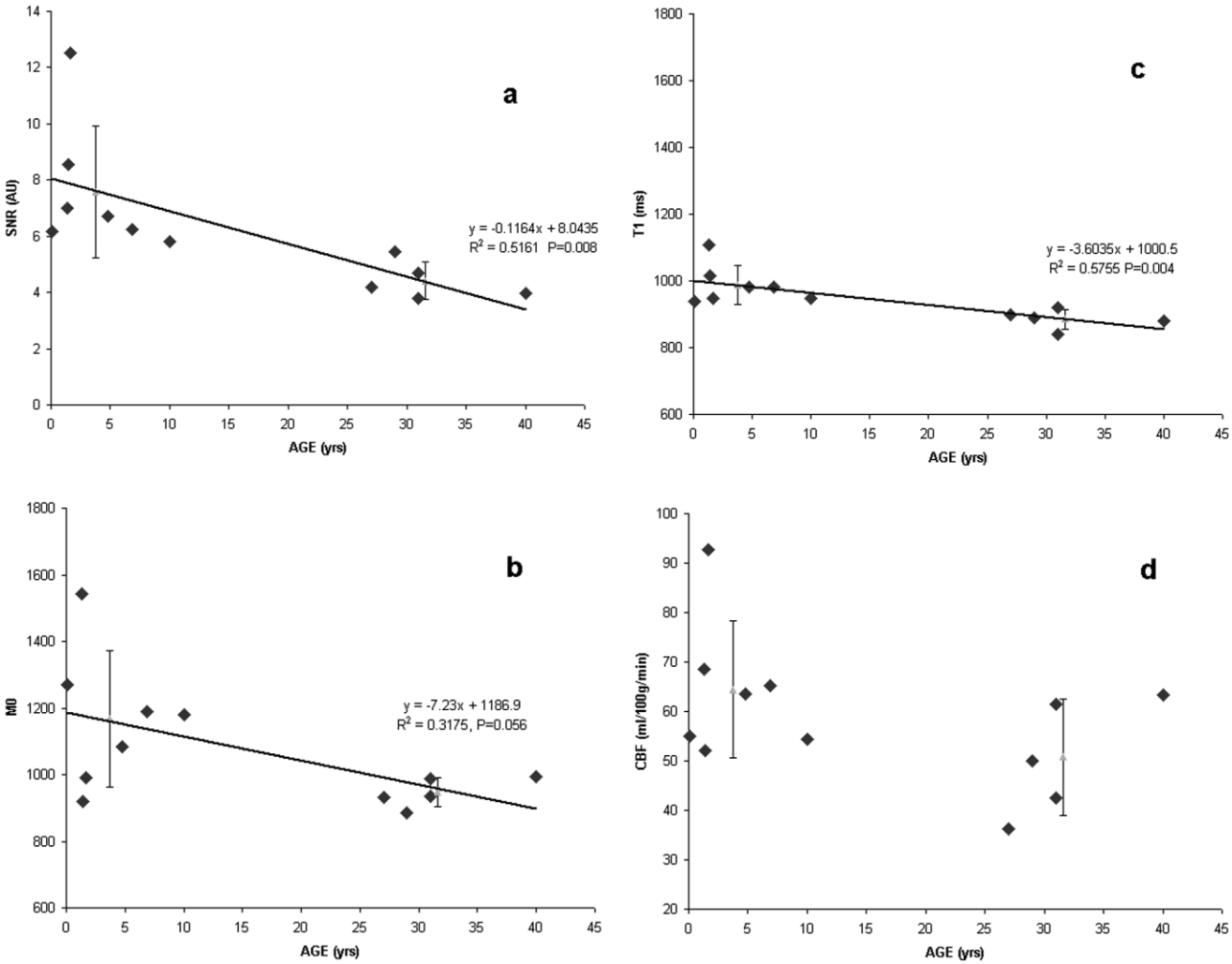

Figure 4. Measures of whole brain based ASL SNR (**a**), M_0 (**b**), T1 (**c**), and CBF (**d**) as a function of age. Except for CBF, the other three parameters show negative linear relationship with age. The fitted function along with the correlation coefficient (R) and *P*-value of the regression analysis are shown in the plots. The triangle symbols and error bars represent the mean and SD, respectively, of the CBF measurements in each group.

by the SD divided by the mean of the time course of ΔM images, was measured in the whole brain, gray matter, and white matter ROIs and compared between the two age groups.

RESULTS

M_0 and T1 Mapping

Figure 2 displays the averaged T1 histogram along with representative T1 and M_0 images from the child and adult group. It can be clearly seen that child brain has both elevated T1 and M_0 compared to adult brain, and the differences reach statistical significance (see Table 1). The averaged T1 histogram shows adult T1s are not only distributed in a relatively lower range, they are also more dispersed compared to the child data. The child T1 values are more concentrated, and the separation between gray and white matter is more difficult to be discerned. Based on Figure 2, the T1 range associated with white and gray matter was empirically defined as 600–800 msec and 800–1100 msec, respectively, in adults, and 650–850 msec and 850–1150 msec, respectively, in children. This T1 based empirical tissue segmentation was verified in each subject by comparison with raw EPI images and ASL perfusion images that showed contrast between the gray and white matter. The volume fraction of white matter was found to be reduced, and the fraction of gray matter was correspondingly increased in children compared to adults (see Table 1). This effect was also statistically significant.

Perfusion Imaging

Figure 3 displays four representative sets of ASL perfusion images acquired at three delays in the child (a, b, c) and adult (d) group. With delay time greater than 0.7 second, most of the bright focal intravascular signal disappears and the cortical structures become manifest in all four data sets. The overall image intensity fades as the delay time increases and also decreases from inferior to superior slices due to the T_1 decay of the tagged spins. The spatial pattern and intensity of the ΔM images as a function of delay time are similar in the two age groups, and are consistent with previous results using various ASL techniques(21,23,24). The child ASL images show less susceptibility artifact in the orbitofrontal region compared to adult images because the sinuses are not fully formed during childhood(16).

It can be easily seen that the child ASL images provide increased signal as well as improved delineation of cortical and subcortical gray matter structures compared to adult images. The measures of ASL SNR and CBF are tabulated in Tables 2 and 3. The ratio of the whole brain ASL SNR acquired in children and adults is 1.72:1 (1.69 and 1.74 in the gray and white matter, respectively). The mean child CBF (whole brain) is 1.27 times of that in adults (1.23 and 1.34 in the gray and white matter, respectively). Because the T1 and M_0 are higher, the increase of ASL SNR in children compared to adults is greater than the increase in CBF. Unpaired *t*-test shows that the child ASL SNR is significantly higher than that of adults,

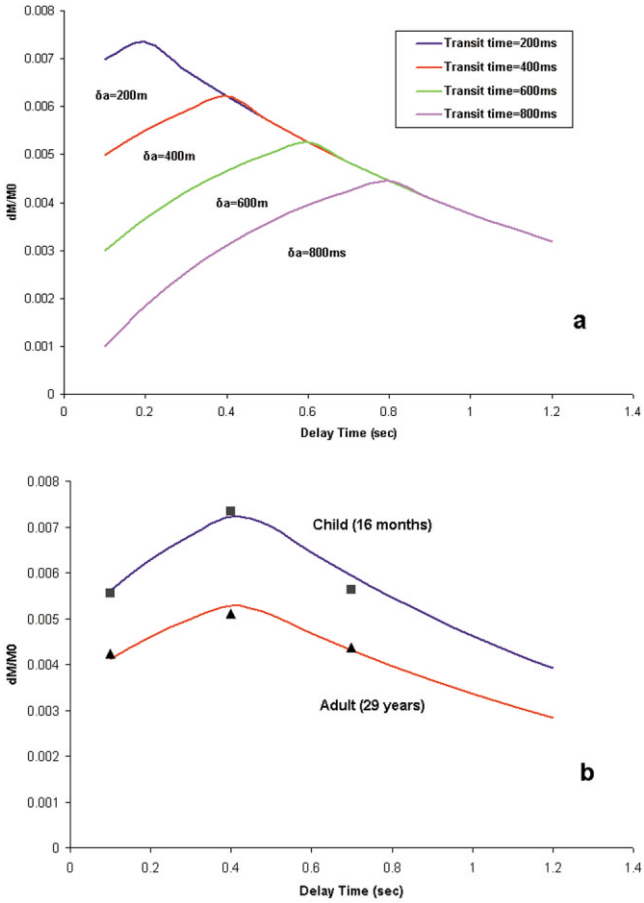

Figure 5. Simulated curve of ASL signal as a function of delay time at various transit times based on Eq. [2] (**a**) and the typical fitted curves in a 16-month-old child and 29-year-old adult (**b**).

while the difference in CBF displays a trend in statistical analysis (Table 3). Figure 4 displays the regression analyses of the whole brain ASL SNR (a), M_0 (b), T1 (c), and CBF (d) with age. The measurements of ASL SNR and T1 showed negative linear relationship with age ($P < 0.05$), whereas the regression of M_0 with age nearly reached statistical significance ($P = 0.056$). The linear regression of CBF with age was not statistically significant.

Figure 5 shows the simulated curve of ASL signal as a function of delay time (a) and the fitted curves in two typical subjects from each age group (b). The transit time estimated from the ASL signal series in the bottom slice was not significantly different between adults and children (see Table 4). The pattern of the fitted curves in Figure 5b suggests that child ASL signal is increased due to prolonged T1, elevated CBF, and M_0 (see Discussion), but the flow velocity seems to remain the same as in adults. Temporal stability characterized by the normalized temporal SD shows no significant change between the two age groups (Table 4). Our results suggest child and adult image series demonstrate similar relative levels of temporal fluctuation due to motion or physiologic noise.

Table 4
Transit Time and Temporal Fluctuation Measured in the Child and Adult Groups

	Transit time (msec)	Temporal fluctuation		
		GM	WM	WB
Child group	481.1 ± 67.1[a]	0.51 ± 0.15	1.43 ± 1.16	0.55 ± 0.17
Adult group	416.2 ± 50.9	0.46 ± 0.22	1.22 ± 0.72	0.55 ± 0.27

[a] $N = 5$.

Clinical Applications

CBF images acquired at the delay time of 700 msec from three children with cerebral disease are shown in Figure 6 (ischemia stroke, 83-month-old male), Figure 7 (benign external hydrocephalus, 17-month-old male), and Figure 8 (periventricular leukomalacia [PVL], 17-month-old male). In all the three pediatric patients, considerable transit related artifacts (bright focal signal) are present, especially in the stroke case, suggesting prolonged transit time. The measured global CBF is markedly lower compared to normal children (36.1, 35.5, and 36.3 mL/100 g/minute for stroke, benign external hydrocephalus, and PVL, respectively). A large area of perfusion deficit is present in the left middle cerebral artery (MCA) territory in the stroke patient, consistent with the infarct location detected in the diffusion-weighted images (DWI). A mismatch between the deficits in the perfusion and diffusion images is also observed, akin to the ischemic penumbra pattern in adult stroke (Fig. 6)(25). The child with benign external hydrocephalus shows not only globally reduced blood flow, but the ventricles are also considerably enlarged, which can be identified in both CBF and T2-weighted images (Fig. 7). PVL, characterized as periventricular white matter ischemic injury, is clearly manifested in the T2-weighted images, especially in the center slice (Fig. 7). Correspondingly, hypoperfusion in the center slice of CBF images is present in a radial region with periventricular origin (Fig. 8).

DISCUSSION

The present study demonstrated the feasibility of noninvasive pediatric perfusion imaging based on a PASL technique at 1.5 T. The obtained perfusion images showed substantial improvement in SNR and moderate increase in quantitative CBF compared with healthy adult data acquired using the same hardware. With the current technique, the values of brain T1 and M_0 can be obtained simultaneously without penalty in scan time. Previous MRI studies on brain maturation suggested that there is a rapid decline in the relaxation time within the first year of life, followed by a more gradual decrease afterwards, especially in white matter(14,26). In neonates, the T1 in white matter can even exceed T1 in gray matter. This phenomenon can be primarily attributed to a decreasing water content, as well as the process of myelination during brain maturation. Our results showing that the measures of brain T1 and M_0 decrease linearly with age are consistent with these findings. Interestingly, the T1 images of the only neonate in the present study showed spatial pattern and value analagous to the older children, with the T1 of gray matter greater than that of white matter. This observation justfied our empirical approach to use uniform T1 range for gray white matter differentiation in the present cohort. The increased ratio of gray vs. white matter volume in children compared to adults has also been reported(27), and has been primarily attributed to changes in cortical cell-packing density and the growth of cortical-subcortical fiber systems after birth(26).

The perfusion model (Eq. [1]) used in this study was based on parameters derived from healthy adults, and might cause errors for child CBF estimation. This possibility arises from the choice of two parameters: the T1 of blood (T_{1a}) and blood–brain partition coefficient of water (λ). Blood T1 in children is expected to be longer than 1.2 seconds because the blood water content is

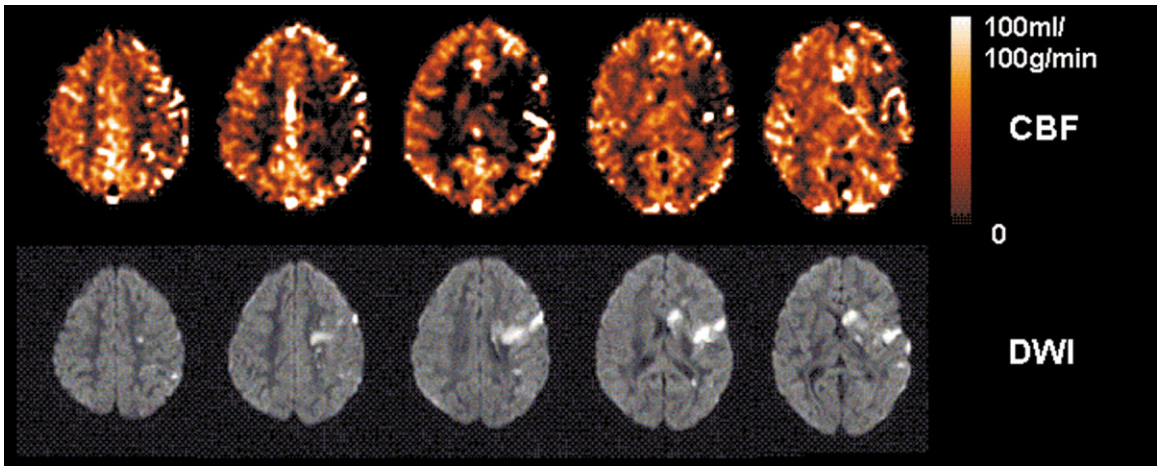

Figure 6. Quantitative CBF and DWI of an 83-month-old boy with ischemic stroke.

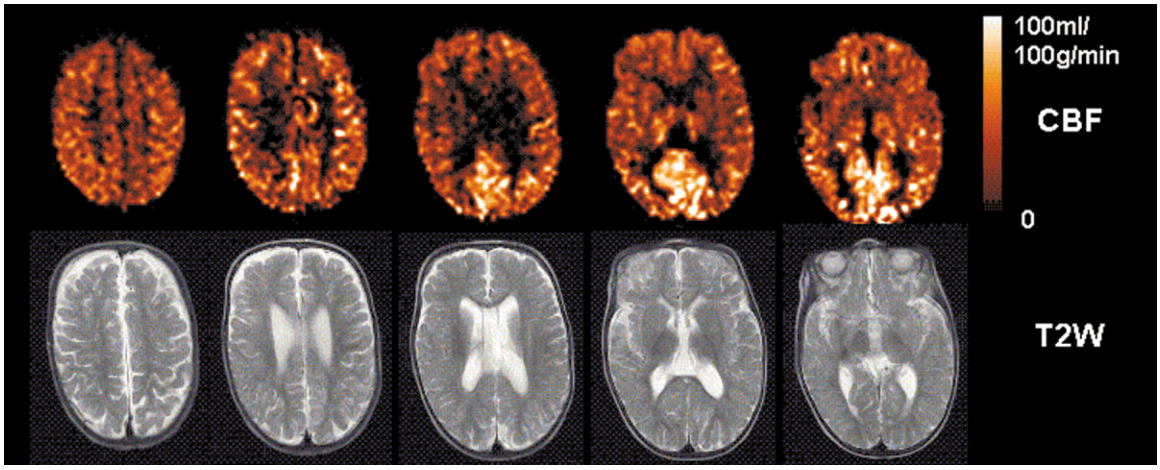

Figure 7. Quantitative CBF and T2-weighted images of a 17-month-old boy with hydrocephalus.

higher than that in adults(28). Our observation of elevated child brain T1 added support to this speculation because it has been reported that blood T1 generally parallels but is slightly higher than brain T1(29). As a result, adopting adult blood T1 in Eq. [1] may lead to overestimation of child CBF. On the other hand, previous results suggested that the blood–brain partition coefficient of water is higher in children (1.1 mL/g in neonates)(28) as opposed to adults (0.9 mL/g), which would cause underestimation of child CBF by using the adult λ. Because the effects of λ and T_{1a} tend to be balanced by each other, the adult perfusion model likely provided a reasonable approximation in child CBF quantification, yielding CBF measures comparable to values obtained using radioactive methods(6). A simulation was carried out to estimate the effects of increased λ and T_{1a} in children on the accuracy of pediatric perfusion quantification. Figure 9 displays the contour map of the deviation between the realistic and calculated CBF values if adult parameters are used in Eq. [1]. Based on the reported values of λ = 1.1 mL/g and $T_{1a} \approx 1.5$ seconds in neonates(28,30), there may be slight (10%) overestimation of perfusion in neonates but the overall error is around 5% across the entire age span (0–18 years). Given the relatively sparse literature and large variability of these parameters in pediatric age groups, CBF quantification based on adult perfusion model seems to be a reasonable solution at present. Nevertheless, optimizing the specific perfusion model for child populations bears considerable importance and significance in clinical diagnosis, as these parameters may vary with pathologic state.

The improvements in the quality of pediatric perfusion images can be attributed to combined effects of increased blood flow, M_0, and T1 in the pediatric population. Because ASL techniques rely on arterial blood water as an endogeous tracer, increased blood water signal (blood M_0) will directly lead to higher tracer quantity and subsequently greater ASL signal in children. Because the lifetime of the tracer determined by blood T1 is also prolonged in children, the loss of spin labeling during the transit time will also be reduced compared to adults, producing further increased perfusion signal in brain tissue. These two effects, in conjunction with the moderately elevated CBF, yield major improvements in the pediatric perfusion signal obtained with ASL MRI.

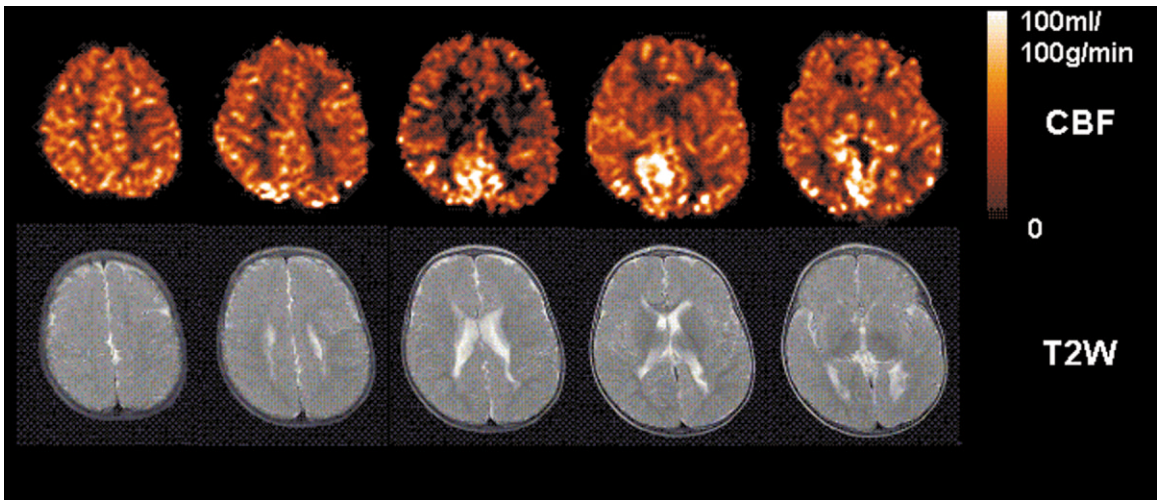

Figure 8. Quantitative CBF and T2-weighted images of a 17-month-old boy with periventricular leukomalacia.

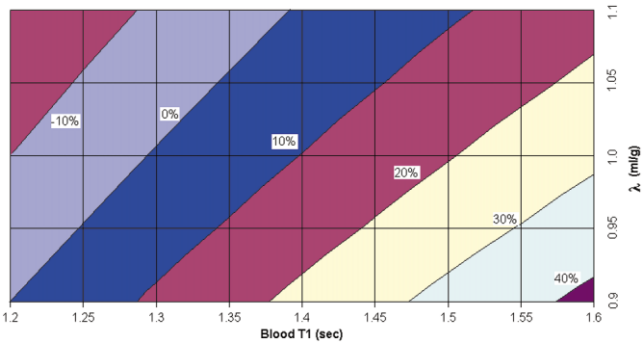

Figure 9. Contour map indicates the simulation results of the effects on pediatric perfusion quantification by using adult parameters of blood T1 and blood brain partition coefficient of water (λ). The realistic CBF is calculated based on Eq. [1] with assumed pediatric parameters of blood T1 and λ as listed in the figure. The percentage deviation between the calculated and realistic CBF is listed beside each contour curve.

Additionally, T2 has been reported to be longer in children than adults(14), which could lead to further advantage in the ASL SNR, although this T2 effect is expected to be small because the T2 of blood at 1.5 T is much longer than (> three times) the current TE of 29 msec. Another interesting observation was that the temporal fluctuation of the ASL image series was at a similar level in both the child and adult groups. This finding does indicate an increased absolute level of signal fluctuation, probably due to greater motion and cardiorespiratory pulsatility in children(16); however, the normalized temporal SD remains the same as in adults because the ASL signal is also increased in children. Because ASL perfusion data are obtained using pair-wise subtraction of control and labeled images on a very short time scale of only a few seconds, bulk motion effects are reduced compared to dynamic susceptibility contrast (DSC) approaches, providing a potentially additional benefit for performing ASL vs. DSC in pediatric subjects.

Previous studies have used radioactive methods such as PET and SPECT to study the developmental change of CBF with age(6,7,9–12). As previously reviewed(8), these studies seem to suggest that child CBF starts at a low level during the perinatal period and peaks around three to eight years before gradually reaching the adult value. Evidence also indicated that there may be intermittent stages of increased CBF corresponding to phases of rapid brain growth during childhood(8). A similar developmental curve of CBF change with age was also observed in rodent studies(31). Interestingly, the observed ratio (1.3) of CBF in the child vs. adult group was highly compatible with previous studies(6,7). However, we were unable to provide a more detailed developmental curve of CBF in the pediatric population because of a relatively small sample size. In the present study, five of the seven children were sedated during CBF measurements. The effects of sedation on child brain metabolism, including CBF, cerebral blood volume, and oxygen consumption are complicated and not well understood. A general trend of suppressed cerebral metabolism during anesthesia has been reported in humans and animals(32,33). CBF in awake children could be higher than the values reported here.

In conclusion, we have demonstrated the feasibility of pediatric perfusion imaging with ASL in children with and without cerebral disease. The improvements in image quality and patient safety render pediatric ASL a very promising approach in diagnosis and prognosis of childhood brain disorders.

ACKNOWLEDGMENTS

This research was partly supported by W.W. Smith Charitable Trust (H0203) and a Pfizer Scholarship to D.J.L.

REFERENCES

1. Ostergaard L, Weisskoff RM, Chesler DA, et al. High resolution measurement of cerebral blood flow using intravascular tracer bolus passages. Part I: mathematical approach and statistical analysis. Magn Reson Med 1996;36:715–725.
2. Detre JA, Zhang W, Roberts DA, et al. Tissue specific perfusion imaging using arterial spin labeling. NMR Biomed 1994;7:75–82.
3. Detre JA, Alsop DC, Vives LR, et al. Noninvasive MRI evaluation of cerebral blood flow in cerebrovascular disease. Neurology 1998;50:633–641.
4. Alsop DC, Detre JA, Grossman M. Assessment of cerebral blood flow in Alzheimer's disease by spin-labeled magnetic resonance imaging. Ann Neurol 2000;47:93–100.
5. Chalela JA, Alsop DC, Gonzalez-Atavalez JB, et al. Magnetic resonance perfusion imaging in acute ischemic stroke using continuous arterial spin labeling. Stroke 2000;31:680–687.
6. Chiron C, Raynaud C, Maziere B, et al. Changes in regional cerebral blood flow during brain maturation in children and adolescents. J Nucl Med 1992;33:696–703.
7. Takahashi T, Shirane R, Sato S, et al. Developmental changes of cerebral blood flow and oxygen metabolism in children. AJNR Am J Neuroradiol 1999;20:917–922.
8. Epstein HT. Stages of increased cerebral blood flow accompany stages of rapid brain growth. Brain Dev 1999;21:535–539.
9. Schoning M, Hartig B. Age dependence of total cerebral blood flow volume from childhood to adulthood. J Cereb Blood Flow Metab 1996;16:827–833.
10. Chugani HT, Phelps ME. Maturational changes in cerebral function in infants determined by 18FDG positron emission tomography. Science 1986;231:840–843.
11. Ogawa A, Sakurai Y, Kayama T, et al. Regional cerebral blood flow with age: changes in rCBF in childhood. Neurol Res 1989;11:173–176.
12. Barthel H, Wiener M, Dannenberg C, et al. Age-specific cerebral perfusion in 4- to 15-year-old children: a high-resolution brain SPET study using 99mTc-ECD. Eur J Nucl Med 1997;24:1245–1252.
13. Dobbing J, Sands J. Quantitative growth and development of human brain. Arch Dis Child 1973;48:757–767.
14. Holland BA, Haas DK, Norman D, et al. MRI of normal brain maturation. AJNR Am J Neuroradiol 1986;7:201–208.
15. Wong EC. Potential and pitfalls of arterial spin labeling based perfusion imaging techniques for MRI. In: Moonen CTW, Bandettini PA, editors. Functional MRI. Heidelberg: Springer-Verlag; 1999. p 63–69.
16. Gaillard WD, Grandin CB, Xu B. Developmental aspects of pediatric fMRI: considerations for image acquisition, analysis, and interpretation. Neuroimage 2001;13:239–249.
17. Kim SG. Quantification of relative cerebral blood flow change by flow-sensitive alternating inversion recovery (FAIR) technique: application to functional mapping. Magn Reson Med 1995;34:293–301.
18. Wang J, Alsop DC, Li L, et al. Comparison of quantitative perfusion imaging using arterial spin labeling at 1.5 and 4 Tesla. Magn Reson Med 2002;48:242–254.
19. Matson GB. An integrated program for amplitude-modulated RF pulse generation and re-mapping with shaped gradients. Magn Reson Imaging 1994;12:1205–1225.

20. Wong EC, Buxton RB, Frank LR. Quantitative imaging of perfusion using a single subtraction (QUIPSS and QUIPSS II). Magn Reson Med 1998;39:702–708.
21. Alsop DC, Detre JA. Reduced transit-time sensitivity in noninvasive magnetic resonance imaging of human cerebral blood flow. J Cereb Blood Flow Metab 1996;16:1236–1249.
22. Siemens MAGNERTON Vision manual. Functional description 2, Siemens AG, 1993.
23. Gonzalez-At JB, Alsop DC, Detre JA. Perfusion and transit time changes during task activation determined with steady-state arterial spin labeling. Magn Reson Med 2000;43:739–746.
24. Edelman RR, Siewert B, Darby DG, et al. Qualitative mapping of cerebral blood flow and functional localization with echo-planar MR imaging and signal targeting with alternating radio frequency. Radiology 1994;192:513–520.
25. Touzani O, Roussel S, MacKenzie ET. The ischaemic penumbra. Curr Opin Neurol 2001;14:83–88.
26. Inder TE, Huppi PS. In vivo studies of brain development by magnetic resonance techniques. Ment Retard Dev Disabil Res Rev 2000;6:59–67.
27. Giedd JN, Blumenthal J, Jeffries NO, et al. Brain development during childhood and adolescence: a longitudinal MRI study. Nat Neurosci 1999;2:861–863.
28. Herscovitch P, Raichle ME. What is the correct value for the brain–blood partition coefficient for water? J Cereb Blood Flow Metab 1985;5:65–69.
29. Rooney WD, Johnson G, Tanabe J, et al. Relaxometric relaxographic imaging of human brain. In: Proceedings of the 7th Annual Meeting of ISMRM, Philadelphia, 1999. p 609.
30. van der Knaap MS, Valk J. MR imaging of the various stages of normal myelination during the first year of life. Neuroradiology 1990;31:459–470.
31. Rowan RA, Maxwell DS. Patterns of vascular sprouting in the postnatal development of the cerebral cortex of the rat. Am J Anat 1981;160:247–255.
32. Theodore WH. The role of fluorodeoxyglucose-positron emission tomography in the evaluation of seizure disorders. Semin Neurol 1989;9:301–306.
33. Todd MM, Weeks J. Comparative effects of propofol, pentobarbital, and isoflurane on cerebral blood flow and blood volume. J Neurosurg Anesthesiol 1996;8:296–303.